

# Optical properties of paramagnetic ion-doped semiconductor nanocrystals

A. K. Bhattacharjee

*Laboratoire de Physique des Solides, UMR du CNRS, Université Paris-Sud, 91405 Orsay, France*

J. Pérez-Conde

*Departamento de Física, Universidad Pública de Navarra, E-31006 Pamplona, Spain*

(Received 30 January 2003; revised manuscript received 2 May 2003; published 3 July 2003)

We present a theoretical study of the optical properties of quantum dots containing a single paramagnetic ion. The eigenvalue problem of an electron-hole pair in interaction with a localized spin is solved. In Mn-doped nanocrystals of II-VI semiconductors such as CdTe the fundamental absorption line splits into six components, whose relative intensities strongly depend on the Mn spin orientation with respect to the polarization of light, suggesting the possibility of optical detection of spin. With the Mn atom at the center of the quantum dot the overall zero-field splitting is typically an order of magnitude larger than the saturation Zeeman splitting in the bulk diluted magnetic semiconductor with the same average concentration of Mn. The effects of an applied magnetic field are also investigated and recently reported magnetic circular dichroism data in high-quality ZnSe:Mn nanocrystals is discussed.

DOI: 10.1103/PhysRevB.68.045303

PACS number(s): 78.67.Bf, 71.70.Gm, 75.50.Pp

## I. INTRODUCTION

The current interest in paramagnetic ion-doped nanocrystals (NC's) is related to their possible applications in spintronics and quantum information processing. A voltage-controlled spin filter based on a semiconductor NC with a single spin has been recently proposed.<sup>1</sup> The optical injection of carriers in such a quantum dot (QD) also seems promising for the detection and manipulation of individual spins. Small-size Mn-doped ZnS NC's were early synthesized by Bhargava *et al.*,<sup>2</sup> who studied their optical properties with particular emphasis on the Mn photoluminescence. In fact, such NC's belong to the family of semimagnetic or diluted magnetic semiconductors (DMS's), which are known for giant magneto-optical effects arising from the strong *sp-d* exchange interactions between the band carriers and the transition-metal ions. However, the Zeeman shift of the photoluminescence excitation (PLE) band edge at 1.6 K in the ZnS:Mn NC's in a magnetic field of 4.5 T was found to be much smaller (less than 5 meV) than in the bulk DMS of comparable average Mn concentration. Recently, Hoffman *et al.*<sup>3</sup> reported magnetic circular dichroism (MCD) measurements in CdS:Mn NC's. They pointed out that a huge exciton splitting (even in zero field) was expected in a QD with a single Mn at the center, but observed only a saturation Zeeman splitting of 3.2 meV in their sample, about five times smaller than in the corresponding bulk material. More recently, Norris *et al.*<sup>4</sup> obtained a much larger splitting of 28 meV in high-quality Mn-doped NC's of ZnSe. The chemically synthesized NC's studied in Refs. 2–4 were estimated to include a single Mn ion each on the average. Glass-embedded DMS NC's with higher Mn concentrations ( $\sim 10\%$ ) were previously investigated.<sup>5,6</sup> Our early theoretical study<sup>7</sup> focused on the Zeeman effect and the exciton magnetic polaron in such systems. The former, treated in the mean-field approximation, predicted a confinement-induced reduction of the excitonic Zeeman splitting with respect to the bulk, arising from the mixing of the light- and heavy-hole

band states in the hole wave function, in accord with the magnetoabsorption data in  $\text{Cd}_{1-x}\text{Mn}_x\text{Se}$  NC's.<sup>6</sup> An additional reduction of the Zeeman effect in low-dimensional DMS structures is related to the wave vector dependence of the *sp-d* exchange interactions in bulk semiconductors.<sup>8</sup> However, as we shall see in the following, a mean-field approach is inadequate for NC's containing a single magnetic ion. Here, we present a full quantum-mechanical theory of an electron-hole pair (exciton) in interaction with a localized spin and deduce the optical absorption and magnetoabsorption spectra.

## II. THEORY

We consider a spherical QD of radius  $a$  smaller than the bulk exciton Bohr radius  $a_B$ . In this strong confinement regime, neglecting the small excitonic correlation, the lowest-energy states of an electron-hole (*e-h*) pair can be written as

$$\Psi_{m\mu}^{e-h}(\mathbf{r}_e, \mathbf{r}_h) = \psi_m^e(\mathbf{r}_e) \psi_\mu^h(\mathbf{r}_h). \quad (1)$$

Here the electron wave function is

$$\psi_m^e(\mathbf{r}) = \phi(\mathbf{r}) u_m^c(\mathbf{r}), \quad (2)$$

with the  $1s$  envelope function

$$\phi(\mathbf{r}) = \sqrt{\frac{2}{a}} \frac{\sin(\pi r/a)}{r} Y_{00}. \quad (3)$$

$u_m^c(\mathbf{r})$  is the conduction band Bloch function at  $\Gamma$ , with  $m = s_z = \pm \frac{1}{2}$ . In the spherical approximation for the Luttinger Hamiltonian the hole wave functions are<sup>9</sup>

$$\psi_\mu^h(\mathbf{r}) = \sum_\nu F_{\nu\mu}(\mathbf{r}) u_\nu^h(\mathbf{r}), \quad (4)$$

where  $\mu, \nu$  run through  $\frac{3}{2}, \frac{1}{2}, -\frac{1}{2},$  and  $-\frac{3}{2}$ .  $u_\nu^h(\mathbf{r})$  are the time-reversed valence band Bloch functions at  $\Gamma$ , with  $j_z = \nu$ . Note that we have included only the fourfold  $\Gamma_8$  va-

lence bands in Eq. (4), by assuming a large spin-orbit coupling. However, it can be easily extended to include the spin-orbit split-off band  $\Gamma_7$  in semiconductors such as CdS with a small spin-orbit interaction. Here, we consider the dipole-active fourfold ground state  $1S_{3/2}$  that corresponds to

$$F_{\nu\mu}(\mathbf{r}) = \delta_{\nu\mu} R_0(r) Y_{00} + \left\langle \frac{3}{2}, \nu; 2, (\mu - \nu) \left| \frac{3}{2}, \mu \right. \right\rangle \times R_2(r) Y_{2, \mu - \nu}(\theta, \varphi), \quad (5)$$

where Clebsch-Gordan coefficients have been used. The radial functions  $R_0(r)$  and  $R_2(r)$  are linear combinations of spherical Bessel functions  $R_0(r) = C[j_0(kr/a) - \kappa j_0(kr\sqrt{\delta}/a)]$  and  $R_2(r) = -C[j_2(kr/a) + \kappa j_2(kr\sqrt{\delta}/a)]$ . Here  $C$  is the normalization constant,  $\kappa \equiv j_0(k)/j_0(k\sqrt{\delta})$ , with  $k$  given by the lowest solution of  $j_2(k)j_0(k\sqrt{\delta}) + j_0(k)j_2(k\sqrt{\delta}) = 0$ . Note that the hole energy is  $E_0 = \hbar^2(\gamma_1 - 2\gamma)(k/a)^2/(2m_0)$ , where  $\gamma \equiv (2\gamma_2 + 3\gamma_3)/5$ . Also,  $\delta \equiv (\gamma_1 - 2\gamma)/(\gamma_1 + 2\gamma)$ .  $\{\gamma_i\}$  are the Luttinger parameters and  $m_0$  is the free-electron mass.

The exchange interaction between a band electron (spin  $s = \frac{1}{2}$ ) and the Mn  $d$  electrons (total ionic spin  $S = \frac{5}{2}$ ) located at  $\mathbf{R}$  is given by

$$\mathcal{H} = -J(\mathbf{r} - \mathbf{R})\mathbf{s} \cdot \mathbf{S}. \quad (6)$$

We follow the perturbation approach and study its effects on the confined electron and hole ground-state multiplets, by neglecting mixing with other states. Indeed, even in a QD with a substantial number of Mn spins, the spin-interaction induced contraction of the carrier wave functions is really small.<sup>10</sup> The contraction due to the electron-hole Coulomb attraction is also small. Now,

$$\langle \psi_m^e | \mathcal{H} | \psi_n^e \rangle = -\alpha |\phi(R)|^2 \langle m | \mathbf{s} \cdot \mathbf{S} | n \rangle, \quad (7)$$

where  $|m\rangle$  is an eigenstate of  $s_z$  and  $\alpha = \langle u_s | J(\mathbf{r}) | u_s \rangle$ , with  $|u_s\rangle$  for the  $s$ -like orbital wave function. Similarly,

$$\langle \psi_\mu^h | \mathcal{H} | \psi_\nu^h \rangle = -\frac{\beta}{3} \sum_{\lambda, \xi} F_{\lambda, \mu}^*(\mathbf{R}) \langle \lambda | \mathbf{j} \cdot \mathbf{S} | \xi \rangle F_{\xi, \nu}(\mathbf{R}), \quad (8)$$

where  $|\mu\rangle$  is an eigenstate of  $j_z$  ( $j = \frac{3}{2}$ ) and  $\beta = \langle u_x | J(\mathbf{r}) | u_x \rangle$ . The Mn spin is described in terms of the  $S_z = M_S$  eigenstates.

While the electron-Mn coupling has the isotropic form  $\mathbf{s} \cdot \mathbf{S}$ , the  $d$  part of the hole envelope function introduces an anisotropy in the hole-Mn coupling in the case of an off-center Mn site. It shows even in the standard mean-field (MF) treatment of the Zeeman effect where one replaces  $\mathbf{S}$  by  $\langle S_z \rangle \hat{\mathbf{z}}$  so that

$$\langle \psi_\mu^h | \mathcal{H} | \psi_\mu^h \rangle = -\frac{\beta}{3} \langle S_z \rangle \mu |f(R)|^2 \left[ 1 + t(R) \left( \mu^2 - \frac{5}{4} \right) (3 \cos^2 \theta - 1) + t(R)^2 \sum_{\lambda} \lambda C_{\lambda, \mu}^2 |Y_{2, \mu - \lambda}(\theta, \varphi)|^2 \right], \quad (9)$$

where  $C_{\lambda, \mu} \equiv \langle \frac{3}{2}, \lambda; 2, (\mu - \lambda) | \frac{3}{2}, \mu \rangle$ ,  $t(r) = g(r)/f(r)$ ,  $f(r) \equiv R_0(r)/\sqrt{4\pi}$ ,  $g(r) \equiv R_2(r)/\sqrt{4\pi}$ , and  $\mathbf{R} = (R, \theta, \varphi)$ . As usual,  $\langle S_z \rangle$  denotes the thermodynamical average of the spin component along the applied field. Note that  $|t(r)|$  vanishes at the origin and increases rather slowly with  $r$ , while  $f(r)$  decreases. Anyway, the splitting of the hole level is a maximum at  $R = 0$ . If we consider an ensemble of same size QD's each containing one Mn ion at a random position, the average Zeeman splitting in the mean-field approximation will be given by the volume integral of Eq. (9):

$$E_\mu^h = -\rho(1/V)(\beta/3) \langle S_z \rangle \mu, \quad (10)$$

where  $V$  is the QD volume and  $\rho$  is the reduction factor obtained in Ref. 7:  $\rho = \int [f^2(r) + (1/5)g^2(r)] 4\pi r^2 dr$ .

In this paper we shall discuss an exact solution. Clearly, in the general case of an arbitrary position  $\mathbf{R}$  of Mn, the full Hamiltonian including the anisotropic hole-Mn coupling can be handled numerically. We shall, however, focus on the special case of Mn located at the center of the QD, which allows an analytical solution and illustrates the essential physics. The spin interaction Hamiltonian is then given by

$$H = -I_e(\mathbf{s} \cdot \mathbf{S}) - I_h(\mathbf{j} \cdot \mathbf{S}) - I_{eh}(\mathbf{s} \cdot \mathbf{j}), \quad (11)$$

where

$$I_e = \alpha |\phi(0)|^2 = N_0 \alpha (\pi/8) (a_L/a)^3, \quad (12a)$$

$$I_h = (\beta/3) |f(0)|^2 = N_0 \beta (1/12) D(\delta) (a_L/a)^3, \quad (12b)$$

$$I_{eh} = 2\hbar \omega_{ST} \chi(\delta) (a_B/a)^3. \quad (12c)$$

Here  $a_L$  and  $a_B$  are the lattice constant and the bulk exciton Bohr radius, respectively.  $N_0$  is the number of cations per unit volume and  $\hbar \omega_{ST}$  is the singlet-triplet splitting due to the electron-hole exchange interaction.<sup>11</sup> The functions  $D$  and  $\chi$  depend only on the effective-mass ratio  $\delta$  as indicated.

Noting that  $\mathbf{J} = \mathbf{s} + \mathbf{j} + \mathbf{S}$  commutes with  $H$ , the eigenvalues and eigenstates can be deduced analytically by using the theory of addition of three angular momenta. In fact, the good quantum numbers are  $s, j, S, J$ , and  $M = J_z$ . We first add  $\mathbf{s}$  and  $\mathbf{S}$  to obtain  $\boldsymbol{\sigma}_s$ . In nontrivial cases the two values  $\sigma_s = S \pm \frac{1}{2}$  are compatible with a given  $J$ . This leads to a  $2 \times 2$  matrix for a given set of  $(J, M)$ . The matrix elements of  $\mathbf{j} \cdot \mathbf{S}$  are calculated by using the Racah coefficients. The corresponding matrix elements of  $\mathbf{j} \cdot \mathbf{s}$  are simply related to the former. Finally, with  $|1\rangle \equiv |S + \frac{1}{2}, j, J, M\rangle$  and  $|2\rangle \equiv |S - \frac{1}{2}, j, J, M\rangle$  as the basis states, we have the matrix elements:

$$H_{11} = -\frac{I_e}{2} S - \frac{I_h}{2} (U + A) - \frac{I_{eh}}{2} \left( J - S - A - \frac{1}{2} \right), \quad (13a)$$

$$H_{12} = \frac{1}{2} (I_h - I_{eh}) \sqrt{AB}, \quad (13b)$$

$$H_{22} = \frac{I_e}{2} (S + 1) - \frac{I_h}{2} (U + B) - \frac{I_{eh}}{2} \left( J + S - B - \frac{1}{2} \right), \quad (13c)$$

where  $U \equiv J^2 - S(S+1) - (j + \frac{1}{2})^2$ ,  $A \equiv [(j + \frac{1}{2})^2 - (J - S)^2]/(2S+1)$ , and  $B \equiv [(J + S + 1)^2 - (j + \frac{1}{2})^2]/(2S+1)$ . The two energy levels for a given  $J$  are

$$\Lambda_{\pm}^J = \frac{1}{4}(I_e - I_h + I_{eh}) - \frac{I_h}{2} \left[ \left( J + \frac{1}{2} \right)^2 - \left( S + \frac{1}{2} \right)^2 - \left( j + \frac{1}{2} \right)^2 \right] \pm \frac{1}{2} \left[ \left( J + \frac{1}{2} \right)^2 (I_e - I_h)(I_{eh} - I_h) + \left( S + \frac{1}{2} \right)^2 (I_e - I_h)(I_e - I_{eh}) + \left( j + \frac{1}{2} \right)^2 (I_e - I_{eh})(I_h - I_{eh}) \right]^{1/2}. \quad (14)$$

The corresponding eigenstates  $|J, \pm, M\rangle$  are linear combinations of  $|1\rangle$  and  $|2\rangle$ ; the respective coefficients can be calculated from the matrix elements in Eqs. (13) and the eigenvalues. These basis states in turn can be written in terms of the states  $|\frac{1}{2}, m_e\rangle |j, m_h\rangle |S, M_S\rangle$  by using the Clebsch-Gordan coefficients, completing our solution of the exciton-Mn eigenvalue problem.

In the present case of  $S = 5/2$  and  $j = 3/2$ , we have a total of eight energy levels:  $J = 1/2(1)$ ,  $3/2(2)$ ,  $5/2(2)$ ,  $7/2(2)$ ,  $9/2(1)$ , where the number in parenthesis shows the number of levels. Note that the 2 levels  $J = 1/2$  and  $J = 9/2$  are electric-dipole forbidden for optical transitions, because they have no projection of the dipole active  $j_{\text{ex}} = 1$  exciton states

$$|1, 1\rangle = -\frac{1}{2} \left| \frac{1}{2}, \frac{1}{2} \right\rangle \left| \frac{3}{2}, \frac{1}{2} \right\rangle + \frac{\sqrt{3}}{2} \left| \frac{1}{2}, -\frac{1}{2} \right\rangle \left| \frac{3}{2}, \frac{3}{2} \right\rangle, \quad (15a)$$

$$|1, 0\rangle = -\frac{1}{\sqrt{2}} \left| \frac{1}{2}, \frac{1}{2} \right\rangle \left| \frac{3}{2}, -\frac{1}{2} \right\rangle + \frac{1}{\sqrt{2}} \left| \frac{1}{2}, -\frac{1}{2} \right\rangle \left| \frac{3}{2}, \frac{1}{2} \right\rangle, \quad (15b)$$

$$|1, -1\rangle = -\frac{\sqrt{3}}{2} \left| \frac{1}{2}, \frac{1}{2} \right\rangle \left| \frac{3}{2}, -\frac{3}{2} \right\rangle + \frac{1}{2} \left| \frac{1}{2}, -\frac{1}{2} \right\rangle \left| \frac{3}{2}, -\frac{1}{2} \right\rangle, \quad (15c)$$

which correspond to optical injection by light of polarization  $\sigma_+$ ,  $\pi$ , and  $\sigma_-$ , respectively.

Typically, the electron-hole exchange  $I_{eh}$  is much smaller than either of the carrier-ion coupling parameters  $I_e$  and  $I_h$ . Also,  $I_e(I_h)$  is positive (negative). Thus, the ground state of the coupled spin-exciton system is the lower level ( $\Lambda_-^J$ ) of  $J = S - 1$ , with the ion spin aligned parallel to the electron spin and antiparallel to the hole angular momentum. Similarly, the highest energy level is the upper level ( $\Lambda_+^J$ ) of  $J = S + 1$ , with the opposite spin alignments. The energy difference between these two levels is the overall zero-field splitting of the exciton:

$$\Delta = -I_h(2S+1) + \frac{1}{2} \left\{ \left[ \left( S + \frac{1}{2} \right) I_e - \left( S + \frac{3}{2} \right) I_h \right]^2 + 3I_e I_h \right\}^{1/2} + \frac{1}{2} \left\{ \left[ \left( S + \frac{1}{2} \right) I_e - \left( S - \frac{1}{2} \right) I_h \right]^2 + 3I_e I_h \right\}^{1/2}. \quad (16)$$

For large  $S$  values it reduces to the classical limit:  $\Delta_{\text{cl}} = S(I_e - 3I_h)$ .

In order to deduce the optical absorption spectrum, let us note that the initial state of the system is that of the paramagnetic ion spin, with the QD valence-band states fully occupied. The spin state can be either a prepared pure (coherent) state or a mixed state describing thermodynamic equilibrium. In either case it can be treated in terms of the eigenstates of  $S_z$ . Thus, without any loss of generality, we consider  $|i\rangle = |M_S\rangle$  for the initial state. By neglecting the magnetic dipole interaction with the electromagnetic field, the spin state remains unchanged in optical transitions. On the other hand, the possible final states  $|f\rangle$  are the eigenstates of  $H$  deduced above. It is easy to see that, in the electric dipole approximation, the relative oscillator strengths of the six allowed transitions are

$$P^{J\pm}(m) = |\langle J, \pm, M | m, M_S \rangle|^2, \quad (17)$$

where  $|m, M_S\rangle \equiv |1, m\rangle |M_S\rangle$  with the  $j_{\text{ex}} = 1$  exciton states in Eqs. (15), the  $m$  values characterizing the polarization of light. Note that the final state  $M = m + M_S$ .

It is interesting to notice that, in the effective-mass approximation (EMA) adopted here, all the spin coupling parameters in Eqs. (12) have the same size dependence: They are inversely proportional to the QD volume. As a result, the exciton-Mn energy levels scale accordingly, but the relative intensities of absorption, depending on the matrix element ratios, remain unchanged.

In the presence of an external magnetic field, in addition to the spin Hamiltonian  $H$  of Eq. (11), we have the Zeeman terms given by

$$H_Z = \mu_{BG_{\text{Mn}}} \mathbf{S} \cdot \mathbf{B} + \mu_{BG_e} \mathbf{s} \cdot \mathbf{B} - \mu_{BG_h} \mathbf{j} \cdot \mathbf{B}. \quad (18)$$

As will be seen below, the resulting Zeeman splittings of the zero-field energy levels are relatively small.

### III. NUMERICAL RESULTS AND DISCUSSION

Motivated by the experimental data of Ref. 4, we present some numerical results for ZnSe QD's. We have neglected  $I_{eh}$  as the singlet-triplet splitting of the bulk exciton is smaller than 0.1 meV.<sup>12</sup> The valence band parameters are  $\gamma_1 = 4.32$ ,  $\gamma_2 = 0.66$ , and  $\gamma_3 = 1.13$ , yielding the ratio  $\delta = 0.393$ , which determines the hole envelope function. It is important to note that, as usual, the EMA grossly overestimates the confinement energies in the QD's investigated in Ref. 4. Nevertheless, tight-binding calculations<sup>13</sup> which correctly reproduce the experimental energy gaps show that the EMA wave functions are relatively accurate in QD's of diameter  $\sim 30$  Å or larger, thus justifying our approach in the present work. As for the carrier-Mn exchange parameters, we have taken the values  $N_0\alpha = 0.29$  eV and  $N_0\beta = -1.4$  eV, measured<sup>14</sup> in bulk  $\text{Zn}_{1-x}\text{Mn}_x\text{Se}$ . The electron  $g$  factor is assumed to have the bulk conduction band value  $g_e = 1.2$ . Then we have  $g_h = -0.86$  from the experimental value<sup>4</sup> of the excitonic Zeeman splitting in the undoped NC's.

Figure 1 shows the zero-field splitting pattern for a ZnSe QD of diameter 29 Å with a single Mn spin at the center.

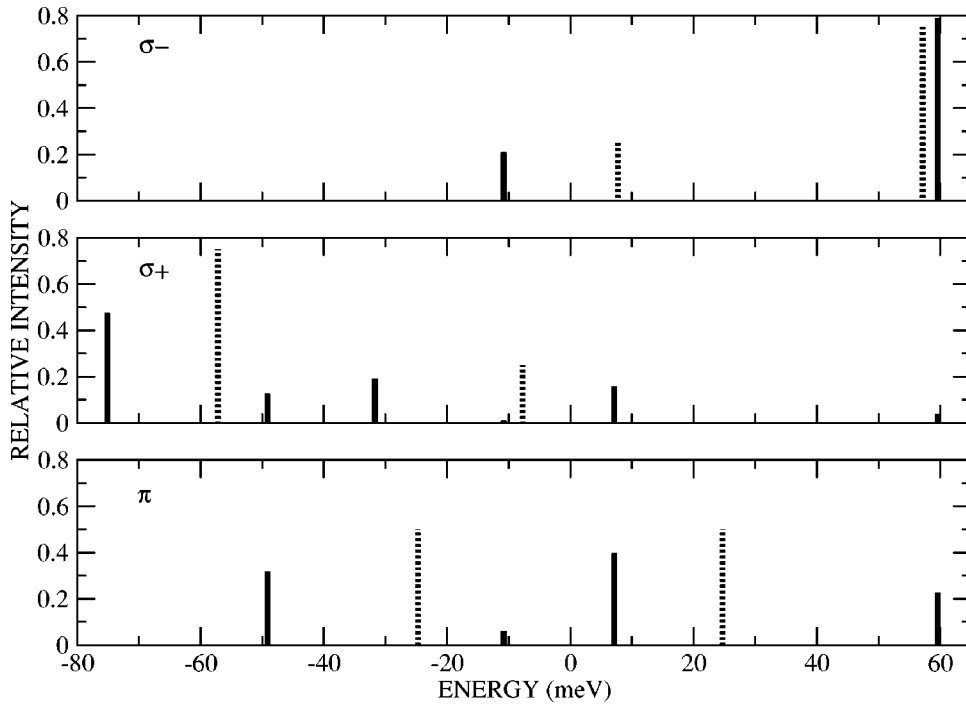


FIG. 1. Splitting of the excitonic absorption in a ZnSe nanocrystal of diameter 29 Å with a Mn impurity at the center with its spin oriented antiparallel to the  $z$  axis ( $M_S = -5/2$ ). The upper two panels, respectively, correspond to  $\sigma_-$  and  $\sigma_+$  circular polarizations (Faraday configuration), while the lowest one corresponds to the  $\pi$  polarization (Voigt configuration). The zero of energy is the spin-independent fundamental gap of the NC. The solid (broken) bars represent the exact (mean-field) results.

Here  $I_e = 6.80$  meV and  $I_h = -12.97$  meV. The relative oscillator strengths shown in this figure assume a pure (prepared) initial state  $M_S = -5/2$ . The upper two panels correspond to the  $\sigma_-$  and  $\sigma_+$  circular polarizations of light, respectively, with respect to the  $z$  axis (direction of propagation). The bottom panel corresponds to the  $\pi$  polarization along  $z$  (Voigt configuration). The solid bars show the results of our exact quantum mechanical solution [see Eqs. (14) and (17)]. The broken bars correspond to a mean-field approach<sup>3</sup> where  $\mathbf{S}$  is treated as a classical vector, with the energy levels given by  $E_{m_e, m_h} = -(I_e m_e + I_h m_h) S$ . It can be seen that the predicted splitting patterns are strikingly different in the two approaches. Notice the large asymmetry of the exact spectra with respect to the zero of energy. Also, the splitting between the strongest  $\sigma_-$  and  $\sigma_+$  components in the exact spectra ( $\approx 135$  meV) is about 18% larger than that ( $\approx 114$  meV) in the MF spectra. Note that the former value checks with  $\Delta$  from Eq. (16) and the latter with its classical limit  $\Delta_{cl}$ . Clearly, by symmetry, if the Mn spin is initially oriented in the opposite direction, i.e.,  $M_S = +5/2$ , the panels for the  $\sigma_+$  and  $\sigma_-$  polarizations get interchanged. Thus the characteristic absorption spectra for the opposite circular polarizations could, in principle, be used for detecting the initial spin orientation of the paramagnetic ion. However, at this point, only MCD experiments seem feasible, measuring simply the overall splitting between the strongest components of  $\sigma_-$  and  $\sigma_+$ . The sign of the splitting would then identify the orientation of the Mn spin. Note that the strongest component in the topmost panel corresponds to the highest energy level, with the exciton spin parallel to the Mn spin, while that in the second panel corresponds to the lowest level, with the exciton spin antiparallel to the Mn spin. This results from the negative (antiferromagnetic) sign of the hole-ion spin interaction.

Figure 2 shows results for an ensemble of 53 Å diameter

ZnSe QD's in thermodynamic equilibrium, each with a Mn spin at the center. In the present case  $I_e = 1.114$  meV,  $I_h = -2.125$  meV, and  $\Delta = 22.1$  meV. The bottom panel corresponds to the case of zero field with randomly oriented Mn spin ( $\langle S_z \rangle = 0$ ) where all light polarizations are equivalent. Note that the same relative intensities hold for the 29 Å QD's with the energy scale modified. The upper two panels show the results for  $\sigma_-$  and  $\sigma_+$  polarizations in the Faraday configuration with  $B = 1$  T along the  $z$  axis. In the presence of an external field,  $J$  is no longer a good quantum number but  $M = J_z$  is. This simplifies<sup>7</sup> the numerical diagonalization of the full Hamiltonian  $H + H_Z$ . For calculating the relative intensities we have assumed  $T = 1.5$  K. In the present case only the applied field breaks the time-reversal symmetry and gives rise to the circular birefringence or dichroism as indicated by the differences between the upper two panels. It is interesting to note that the energy separation of 22 meV between the strongest components of  $\sigma_-$  and  $\sigma_+$  spectra is almost equal to the overall zero-field splitting ( $\Delta$ ) shown in the bottom panel. This is because the external field amounts to a small perturbation with respect to the much stronger "internal field" due to the  $sp-d$  exchange interactions. Let us mention that the MF approach predicts the Zeeman splitting  $\Delta_{MF} = (I_e - 3I_h) |\langle S_z \rangle| + (g_e + 3g_h) \mu_B B$  which amounts to 13.7 meV in the present case ( $\langle S_z \rangle = -1.84$ ). We have investigated the exact spectra at higher magnetic fields up to 10 T. As  $B$  increases the strongest components of  $\sigma_+$  and  $\sigma_-$  shift to lower energies almost linearly by about 0.2 and 0.3 meV/T, respectively, so that the splitting between them decreases from 22 meV at 1 T to 21 meV at 10 T. Also, the oscillator strengths get more concentrated into these two peaks so that their intensities increase. In fact, the energy shifts are related to the  $g$  factors and the relative intensities depend on the degree of alignment of the Mn spin ( $|\langle S_z \rangle|/S$ ). For instance, at  $B = 2.5$  T, the highest field in

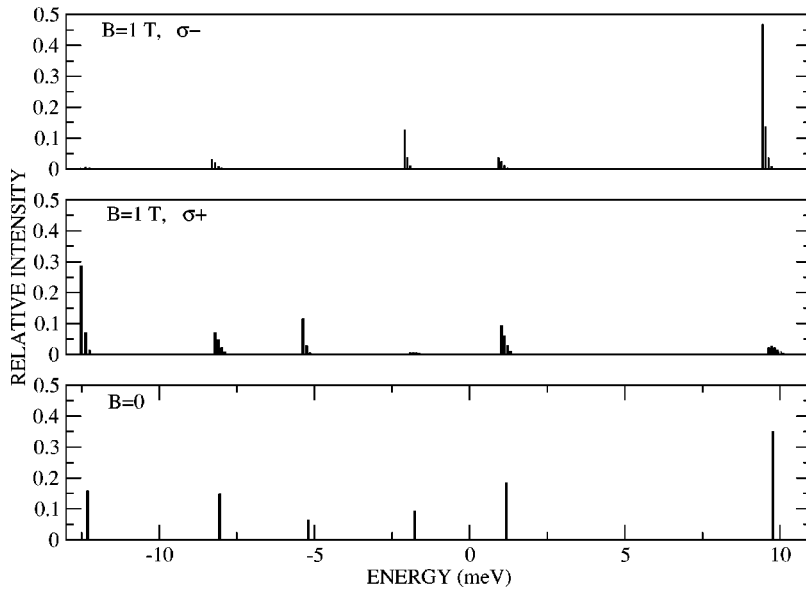


FIG. 2. Splitting of the excitonic absorption in ZnSe nanocrystals of diameter 53 Å, each with a Mn impurity at the center, in thermodynamic equilibrium. The bottom panel shows the zero-field polarization-independent spectrum. The upper two panels respectively correspond to  $\sigma_-$  and  $\sigma_+$  polarizations in an applied field of  $B = 1$  T at  $T = 1.5$  K.

Ref. 4,  $\langle S_z \rangle = -2.38$  and the calculated absorption spectra resemble those in the upper two panels of Fig. 1, except for a slightly enhanced asymmetry due to the energy shifts, with the Zeeman splitting 21.8 meV close to  $\Delta$ . Note that the slow linear decrease of the splitting with increasing  $B$  arises from the negative exciton  $g$  factor. As for the size dependence of the Zeeman splitting, it follows from Eqs. (12) that  $\Delta$  is inversely proportional to the QD volume.

It is satisfying to note that the predicted Zeeman splitting of 22 meV in Mn-doped ZnSe NC's of diameter 53 Å is rather close to the measured value<sup>4</sup> of 28 meV. Notice that no adjustable parameter has been used to deduce this theoretical value. As the Mn impurity was assumed to be located at the center, this is the maximum possible splitting in the case of QD's containing only one Mn. Indeed, for a random position of Mn in the NC, the expected average splitting from Eq. (10) is 2.5 meV only. So, neglecting the uncertainty in the NC size, we can say that the QD's of diameter 53 Å in Ref. 4 contained more than one Mn atom each on the average. On the other hand, the saturation Zeeman splitting 17 (1) meV in the samples of 42 (29) Å size NC's are much smaller than the calculated values 44 (135) meV by assuming Mn at the center. Nevertheless, the observed splitting in the 42 Å NC's is substantially larger than 5 meV expected for a random Mn position. However, that in 29 Å NC's is much smaller than 15 meV expected for a random Mn site. At the estimated doping levels in Ref. 4, the probability of having 2 Mn atoms as antiferromagnetically coupled neighbors in a given NC, which could explain such a decrease,<sup>3</sup> is rather small. The above results, therefore, seem to suggest that the smaller NC's are less likely to incorporate a Mn atom near the center.

The present calculations should be applicable to the QD band-edge photoluminescence provided the energy gap lies

below the Mn fluorescence energy  $\sim 2.1$  eV, because of the relatively fast energy transfer expected from the exciton to the Mn  $d$  shell. Clearly, this condition is not satisfied in the case of ZnSe:Mn NC's, where the absorption gap exceeds 3 eV. But both the excitonic and Mn emissions were observed<sup>4</sup> in the same sample. As the authors pointed out, they need not be originating from the same NC. NC's with a smaller gap such as CdTe:Mn with a stable  $\text{Mn}^{2+}$  ground state of spin  $S = 5/2$  under optical excitation, as assumed here, seem more appropriate for studying spin dynamics and realizing optical manipulation of the localized spin state.

#### IV. CONCLUDING REMARKS

To summarize, we have solved the quantum mechanical problem of an exciton in interaction with a localized spin in a QD and deduced the optical absorption and magnetoabsorption spectra. The results are substantially different than from the mean-field approach used previously. In small-size II-VI compound semiconductor nanocrystals containing a Mn atom at the center, the zero-field splitting of the absorption line is almost an order of magnitude larger than the giant Zeeman splitting at saturation in the corresponding bulk DMS with the same average Mn concentration. Numerical results obtained in the case of ZnSe:Mn NC's show a satisfactory agreement with the recently reported MCD measurements. The theory also provides a basis for further considerations concerning the optical detection and manipulation of a single spin.

#### ACKNOWLEDGMENTS

We wish to thank D. Scalbert for stimulating discussions.

- <sup>1</sup>Al.L. Efros, E.I. Rashba, and M. Rosen, Phys. Rev. Lett. **87**, 206601 (2001).
- <sup>2</sup>R.N. Bhargava, D. Gallagher, X. Hong, and A. Nurmikko, Phys. Rev. Lett. **72**, 416 (1994).
- <sup>3</sup>D.M. Hoffman, B.K. Meyer, A.I. Ekimov, I.A. Merkulov, Al.L. Efros, M. Rosen, G. Couino, T. Gacoin, and J.P. Boilot, Solid State Commun. **114**, 547 (2000).
- <sup>4</sup>D.J. Norris, N. Yao, F.T. Charnok, and T.A. Kennedy, Nano Lett. **1**, 3 (2001).
- <sup>5</sup>Y. Wang, N. Herron, K. Moller, and T. Bein, Solid State Commun. **77**, 33 (1991).
- <sup>6</sup>K. Yanata, K. Suzuki, and Y. Oka, J. Appl. Phys. **73**, 4595 (1993); K. Yanata and Y. Oka, Jpn. J. Appl. Phys. **34**, 164 (1995).
- <sup>7</sup>A.K. Bhattacharjee, Phys. Rev. B **51**, 9912 (1995).
- <sup>8</sup>A.K. Bhattacharjee, Phys. Rev. B **58**, 15 660 (1998).
- <sup>9</sup>P.C. Sercel and K.J. Vahala, Phys. Rev. B **42**, 3690 (1990); Al.L. Efros, *ibid.* **46**, 7448 (1992).
- <sup>10</sup>A.K. Bhattacharjee and C. Benoit à la Guillaume, Phys. Rev. B **55**, 10 613 (1997).
- <sup>11</sup>Al.L. Efros, M. Rosen, M. Kuno, M. Nirmal, D.J. Norris, and M. Bawendi, Phys. Rev. B **54**, 4843 (1996).
- <sup>12</sup>H. E. Gumlich, D. Theis, and D. Tschierse, in *Numerical Data and Functional Relationships in Science and Technology*, edited by O. Madelung, M. Schulz, and H. Weiss, Landolt-Börnstein, New Series, Group III, Vol. 17, Pt. b (Springer-Verlag, Berlin, 1982), p. 126.
- <sup>13</sup>J. Pérez-Conde and A.K. Bhattacharjee, Phys. Rev. B **63**, 245318 (2001).
- <sup>14</sup>A. Twardowski, T. Dietl, and M. Demianiuk, Solid State Commun. **48**, 845 (1983).